DOI:10.1021/jf9031316

JOURNAL OF AGRICULTURAL AND FOOD CHEMISTRY
ARTICLE

Microstructure and Ultrastructure of High-Amylose Rice Resistant Starch Granules Modified by Antisense RNA Inhibition of Starch Branching Enzyme

Cunxu Wei,[†,‡] Fengling Qin,[‡] Lijia Zhu,[†] Weidong Zhou,[§] Yifang Chen,[§] Youping Wang,[‡] Minghong Gu,*[,†] and Qiaoquan Liu*[,†]

[†]Key Laboratories of Crop Genetics and Physiology of the Jiangsu Province and Plant Functional Genomics of the Ministry of Education, [‡]College of Bioscience and Biotechnology, and [§]Center of Measurement, Yangzhou University, Yangzhou 225009, China

A high-amylose transgenic rice line (TRS) modified by antisense RNA inhibition of starch branching enzymes revealed a resistant starch-rich quality. Compound starch granules in whole grains of the regular rice cultivar Teqing (TQ) were readily split during fracturing, whereas the starch granules in TRS were structurally intact and showed large voluminous, non-angular rounded bodies and elongated, filamentous structures tolerant of fracturing. In isolated preparation, TQ starch granules broke up into separate polygonal granules, whereas TRS starch granules kept their intactness. TRS starch granules consisted of packed smaller subgranules, some of which located at the periphery of starch granules were fused to each other with adjacent ones forming a thick band or wall encircling the entire circumference of the granules. TQ starch granules had a high concentration of amylose in the concentric hilum, whereas TRS starch granules showed a relatively even distribution of amylose with intense amylose in both hilum and band.

KEYWORDS: Rice (*Oryza sativa* L.); high-amylose resistant starch granule; microstructure; ultrastructure; semicompound starch granule

INTRODUCTION

Reserve starch is a major source of nourishment for humans and many animals. Most of the starch in the diets of humans is ingested in cooked foods and digested rapidly in the small intestine. However, a variable proportion is not assimilated in the upper gastrointestinal tract. Instead, this fraction, known as resistant starch (RS), reaches the large intestine where it acts as a substrate for fermentation by the microflora that inhabit that region of the gut (*1*). Short chain fatty acids (SCFA) are end products of this fermentation, and these acids are thought to promote the optimal function of the viscera (*2*). Foods high in RS have the potential to improve human health, prevent pathogen infections or diarrhea, and be of benefit in a variety of pathologic processes, such as inflammatory bowel disease (*3*), colon cancer risk (*4*), insulin resistance and diabetes (*5*), and chronic renal or hepatic disease (*6*). The estimated RS intake by Americans is in the range of approximately 3−8 g per person per day (*7*).

The proportion of RS in the diet can be increased by consuming starch that retains granular structures that are naturally more resistant to digestion. This resistance to digestion by raw granules is further increased if the granules have high amylose content (AC). For example, raw high-amylose maize starch is more resistant to digestion than raw wild type maize starch (*8*). Transgenic potato with very-high-amylose tuber starch was produced by antisense inhibition of two starch branching enzymes (SBEs), offered novel properties for both food and nonfood applications (*9*). A high-amylose and RS barley cultivar was proven to have potential health benefits through reduction of plasma cholesterol and production of increased large-bowel SCFA (*10*). High-amylose wheat generated by RNA interference also has a significant potential to improve human health through its RS content (*11*).

Rice is the most important cereal crop and the staple food of over half the world's population. As the primary dietary source of carbohydrates in these populations, rice plays an important role in meeting energy requirements and nutrient intake, but the content of RS in rice is low (*12*). In view of the current concept of nutrition, rice with a higher content of digested starch and a lower content of RS is not the fittest food for health. Breeding for rice high in RS is of particular interest, as it will be easy to incorporate into the dietary-prevention strategy. To address this problem, high-amylose rice breeding is important. Five rice mutant lines (EM10, EM16, EM72, EM129, EM145) with increased AC in starch granules were identified among floury endosperm mutants. The ACs of the mutants ranged from 29.4% to 35.4% (*13*). The rice line Goami 2 was produced by mutagenesis of the *japonica* line Ilpumbeyo, which has approximately twice the proportion of amylose (33% versus 18.6%) (*14*). A rice mutant described RS111 with high RS in hot cooked rice was induced by γ-ray irradiation (*15*).

Thought high-amylose rice starch has been produced from mutants via breeding program, the ACs (< 36%) of these mutant

*Corresponding authors. Tel: +86-514-87996648. E-mail: qqliu@yzu.edu.cn (Q.L.), gumh@yzu.edu.cn (M.G.).

 Published on Web 12/23/2009

rice plants are not very high compared with high-amylose wheat (88.5%) generated by RNA interference (*11*, *13*−*15*). We have generated several very-high-amylose transgenic rice lines by antisense RNA inhibition of SBEs (Zhu et al., manuscript submitted), and these transgenic rice were rich in RS and had been proven to show a significant potential to improve the large bowel health of rat (*16*). In the present study, microstructure and ultrastructure of the granules from a high-amylose RS transgenic rice, as well as its wild type, were investigated and compared with several microscopy techniques, including light microscopy (LM), fluorescent microscopy (FM), confocal laser scanning microscopy (CLSM), scanning electron microscopy (SEM), and transmission electron microscopy (TEM). The detailed structural information from the high-amylose RS should be useful for various applications of high-amylose RS rice in the food and nonfood industry.

MATERIALS AND METHODS

Plant Materials. A transgenic rice line, TRS, with very high amylose and RS content and its wild type Teqing (TQ) were used in this study. TQ is an *indica* rice cultivar with relative high AC, and TRS was generated from TQ after transgenic inhibition of two SBEs (SBEI and SBEIIb) through antisense RNA technique (Zhu et al., manuscript submitted). TRS holds the homozygous transgene and shows the identical growth behavior and plant type as its wild type TQ with the exceptions of the grain composition and starch structure. These two rice lines were simultaneously cultivated in the experimental field of Yangzhou University, Yangzhou, China. The mature grains were used to analyze the microstructure and ultrastructure of starch granules.

Measurement of Amylose and RS Contents. Apparent amylose content (AAC) was determined by using a previously described colorimetric method with iodine−potassium iodide (*17*). RS was measured according to the method of Megazyme RS assay kit (Megazyme, Co. Wicklow, Ireland) (*18*). All analyses were repeated thrice.

Isolation of Starch Granules. Starch granules were isolated following a method described by Takeda et al. (*19*). Briefly, the brown rice was steeped in 0.2% NaOH for 2 days and homogenized in a mortar with a pestle. The homogenate was squeezed through five layers of cotton cloth and then filtered with 100-, 200-, and 400-mesh sieves, successively. The starch was washed with 0.2% NaOH by centrifugation until no biuret reaction occurred and finally washed with water. The precipitated starch was further treated with anhydrous ethanol, dried under atmosphere, ground into powder, and passed through a 100-mesh sieve.

Bright Field Microscopy (BFM) of Iodine-Stained Starch Granules. BFM of iodine-stained starch granules was performed as previously described (*20*). A 5-mg portion of isolated starch was dispersed in 0.25 mL of deionized water, and after dispersion, one drop was placed on the microscope slide. An equal volume of iodine solution was then added before covering with a coverslip. After being stained with iodine for 3 min, the starches on the slide were viewed in the Olympus BX51 BFM equipped with a CCD camera.

Polarized Light Microscopy (PLM) of Starch Granules. Starch granules were examined for the presence of birefringence by using PLM. A specimen was prepared from the mixture of 2 mg of isolated starch and 1 mL of 50% glycerol solution. PLM images were recorded on the Leica DM LM/P polarized light microscopy.

APTS Staining of Starch Granules. A method for visualizing the distribution of amylose and amylopectin in starch granules was developed using the fluorophore APTS (8-amino-1,3,6-pyrenetrisulfonic acid) (*21*). APTS specifically reacts with the reducing end of starch molecules leading to a 1:1 stoichiometric ratio of starch molecule labeling. Because of its smaller size, amylose contains a much higher molar ratio of reducing ends per glucose residue than amylopectin. This results in a higher by-weight labeling of amylose, enabling the distinction of the two molecules by FM and CLSM (*21*). APTS staining was performed essentially as previously described (*21*). Briefly, starch granules (2 mg) were dispersed in 3 μL of freshly made APTS (Molecular Probes) solution (20 mM). Then, 3 μL of 1 M sodium cyanoborohydride was added, and the reaction mixture was incubated at 30 °C for 15 h. The granules were washed 5 times with 1 mL of distilled water and finally suspended in 20 μL of 50% glycerol. The starch granules were fixed in an agar−glycerol matrix and immediately mounted on a glass plate for FM and CLSM analyses.

Table 1. Apparent Amylose and Resistant Starch Contents of Milled Rice[a]

rice materials	apparent amylose content (%)	RS (%)
TQ	22.68 ± 0.07	1.89 ± 0.14
TRS	49.20 ± 0.28	14.92 ± 0.56

[a] All data presented are the means of three repeats ± standard deviation.

FM of APTS-Stained Starch Granules. APTS-stained starch granules were observed with an Olympus BX51 FM equipped with a CCD camera.

CLSM of APTS-Stained Starch Granules. Images of APTS-stained starch granules were recorded on a CLSM (TCS SP2, Leica Microsystems, Germany) as previously described (*21*). A 488 nm laser line was used for excitation, and light was detected in the interval from 500 to 535 nm. Image analysis was performed using the Leica TCS SP2 software and granules were viewed using the "Glow" color scale going from black to red, orange, yellow, and white to represent areas of low to high fluorescence.

Specimen Preparation for SEM. Two types of specimens were prepared for SEM, one for the whole raw grain and the other for the isolated starch granules. For the whole grain, individual mature grain was fractured in the midregion with a razor blade by applying a slight pressure on the top of the grain. During fracturing, efforts were made to produce no physical contact between the razor blade and the fractured surface of the internal endosperm tissues. Fractured rice grains, with the fractured surface upward, were immediately mounted on the specimen stub and sputter-coated with gold before viewing with an environmental scanning electron microscope (ESEM, Philips XL-30) at an accelerating voltage of 20 kV. For isolated starch granules, starch powder was directly mounted on circular aluminum specimen stubs with double-sided sticky tape, sputter-coated with gold, and viewed with the same ESEM as above.

Specimen Preparation for TEM. Isolated starch granules were fixed for 4 h at 0−4 °C with a 1.2% potassium permanganate ($KMnO_4$) solution containing 0.5% sodium chloride (NaCl). After fixation, the starch granules were centrifuged at 3000*g* for 10 min, the supernatant was discarded, and the precipitates were washed 3 times with a 0.5% NaCl solution for 20 min at 0−4 °C and then passed once through 35% ethanol. Samples were further fixed in 70% ethanol for 12 h at 0−4 °C. After the ethanol fixation, samples were successively dehydrated in 80%, 90%, and 100% ethanol at room temperature. Samples were then embedded in low viscosity Spurr's medium. The quality of thin sections was poor due apparently to the nature of starch, so slightly thicker sections (150 nm), which had improved quality compared with the thin sections, were cut with a diamond knife and double stained with 2% aqueous uranyl acetate and lead citrate before being viewed with TEM (Philips Tecnai 12) at 120 kV.

RESULTS

Contents of Amylose and RS. The contents of amylose and RS in rice grains are given in **Table 1**. On the basis of the category classification by the International Rice Research Institute (*22*), starch from TRS should be classified as very-high-amylose starch, which was over twice that from TQ (**Table 1**). The RS content in TRS was significantly higher compared to that of the wild type TQ (**Table 1**).

LM Study of Starch Granules. After being stained with a 0.5% iodine solution, the isolated starch granules from TQ were detected to have regular and polyhedral shape with a size of 3−5 μm under BFM (**Figure 1A**). However, when the purified TRS starch granules were stained with a same (0.5%) iodine solution, they showed so deeply dark that the microstructure was difficult to observe under BFM (**Figure 1B**). So, the TRS starches were stained with a lower (0.125%) iodine solution, and the microstructure could be subsequently clearly observed under BFM (**Figure 1C**). The starch granule shapes of TRS were clearly

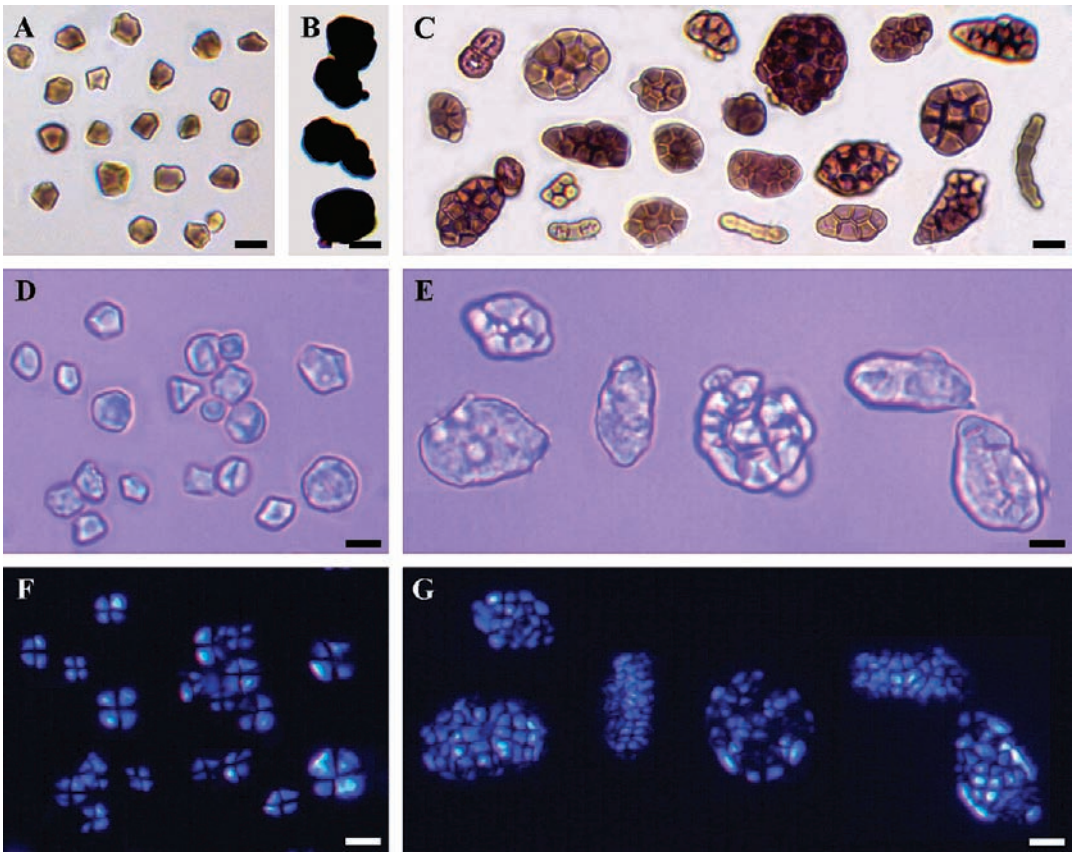

Figure 1. Images of LM. (**A**−**C**) Isolated starch granules stained with iodine solution under BFM: (**A**) starch granules from TQ in 0.5% iodine solution, (**B**) starch granules from TRS in 0.5% iodine solution, (**C**) starch granules from TRS in 0.125% iodine solution. (**D**−**G**) Isolated starch granules without iodine staining under PLM. For each sample, the same field was shown for normal light (**D**, **E**) and polarized light (**F**, **G**): (**D** and **F**) starch granules from TQ, (**E** and **G**) starch granules from TRS. Scale bar = 5 μm.

different from those of TQ; some of the TRS granules were large voluminous, non-angular rounded bodies, which were greatly larger than those of TQ starch granules, and some of the granules were elongated, filamentous structures. Also, the TRS starch granules consisted of many small subgranules but could not break up into the separate subgranules (**Figure 1C**).

When unstained starch granules were observed by PLM with normal bright light, the granule shapes were similar to those stained with iodine solution under BFM (**Figure 1D,E**). All TQ starch granules showed birefringence in the form of the typical maltese crosses by PLM with polarized light, indicating a symmetrical radial molecular orientation in the granules (**Figure 1F**). The large voluminous starch granules of TRS showed many maltese crosses, though each maltese cross was not typical, which showed that TRS starch granules consisted of many subgranules (**Figure 1G**). However, the birefringence of TRS starch granules was considerably weaker, resulting in a lower contrast between birefringence and background compared to TQ starch. Some TRS starch granules, especially elongated and filamentous granules, showed very weak maltese cross (data not shown). This effect would likely be a result of the high amylose concentrations of these starch granules, since amylose molecules were not expected to be specifically uniformly oriented in the granule (*21*). The weak birefringence of TRS starch granules indicated the presence of variations in the molecular orientation of the molecules in the starch granules.

FM Study of Starch Granules. Each starch molecule could be labeled with the fluorophore molecular probe APTS in a nearly 1:1 stoichiometry. Under APTS labeling, the specific internal structures, as well as the general distribution of amylose within the granule could be simultaneously investigated (*21*). After staining with APTS, the TQ starch granules showed evenly bright (**Figure 2A**), whereas TRS starch granules revealed strong staining due to high amylose content at the same exposure time condition of **Figure 2A**; the fluorescent intensity was too strong to observe the microstructure of TRS (data not shown). **Figure 2B** shows the microstructure and fluorescent distribution of TRS starch granules with a shorter exposure time. Large starch granules contained many regularly polygonal subgranules, which were heavily stained (**Figure 2B-①**). Moreover, the band (or wall) encircling the entire circumference of these starch granule was brightly stained too. Both indicated again the high AC in these regions. Besides, some TRS starch granules were internally hollow, but their circumference was also brightly stained (**Figure 2B-②**). Some TRS elongated starch granules revealed multiple highly fluorescent round structures, which appeared to make up the interior of these granules with high amylose (**Figure 2B-③**). **Figure 2C** shows the different focusing plans of a starch granule from **Figure 2C-④**, which presents more clearly the microstructure and amylose distribution in starch granules.

CLSM Study of Starch Granules. CLSM gives a much more comprehensive view of the internal granular structures. CLSM optical sections of TQ starch granules stained with APTS showed an intensely stained centered hilum and no visible growth rings (**Figure 3A1**). CLSM optical sections of TRS starch granules revealed a brightly stained interior and band encircling the entire circumference of the granules, which was consistent with the high AC (**Figure 3A2**−**A6**). The APTS staining pattern of the larger voluminous starch granules revealed that the multiple polygonal subgranules with intensely stained centered hila made up the

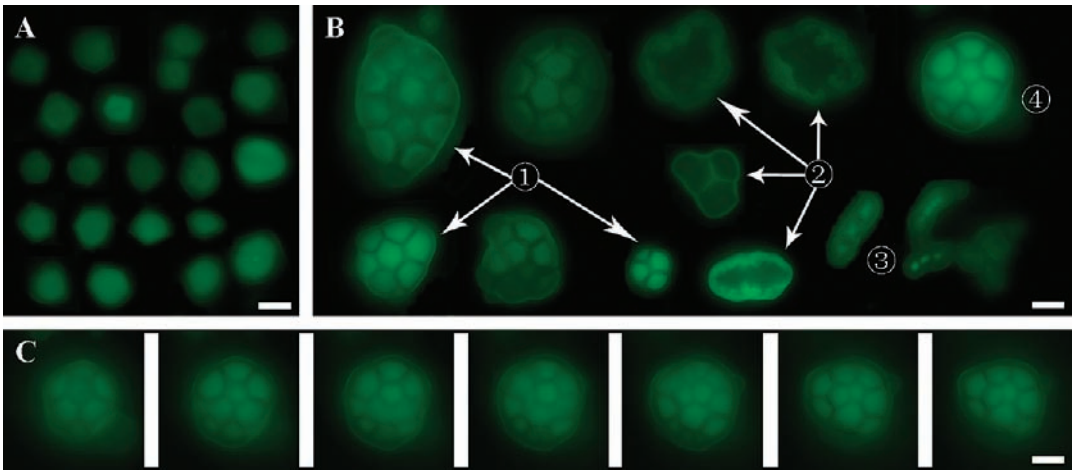

Figure 2. Images of isolated starch granules stained with APTS under FM: (**A**) starch granules from TQ, (**B**) starch granules from TRS, (**C**) different focusing plane of a starch granule shown in **Figure 2B-④**. Scale bar = 5 μm.

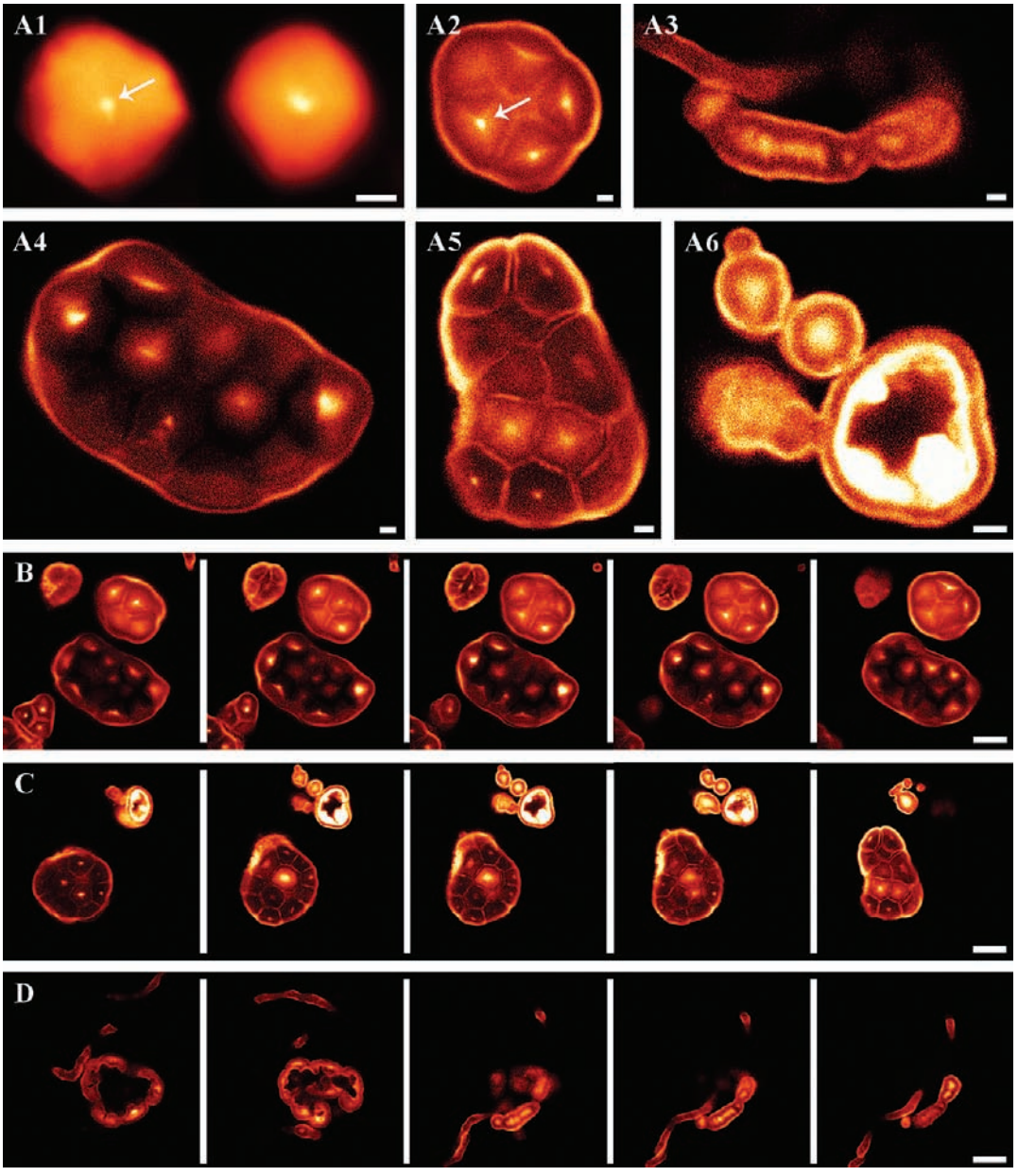

Figure 3. CLSM optical sections of starch granules stained with APTS from TQ (**A1**) and TRS (**A2**−**A6** and **B**−**D**): (**A**) representative CLSM optical slices, showing the hilum and distribution of amylose; (**B**−**D**) serial optical sections of representative TRS starch granules, showing multiple initiations (hila) and the distribution of amylose. Arrow shows hilum. Scale bar = 1 μm for panel **A** and 5 μm for panels **B**−**D**.

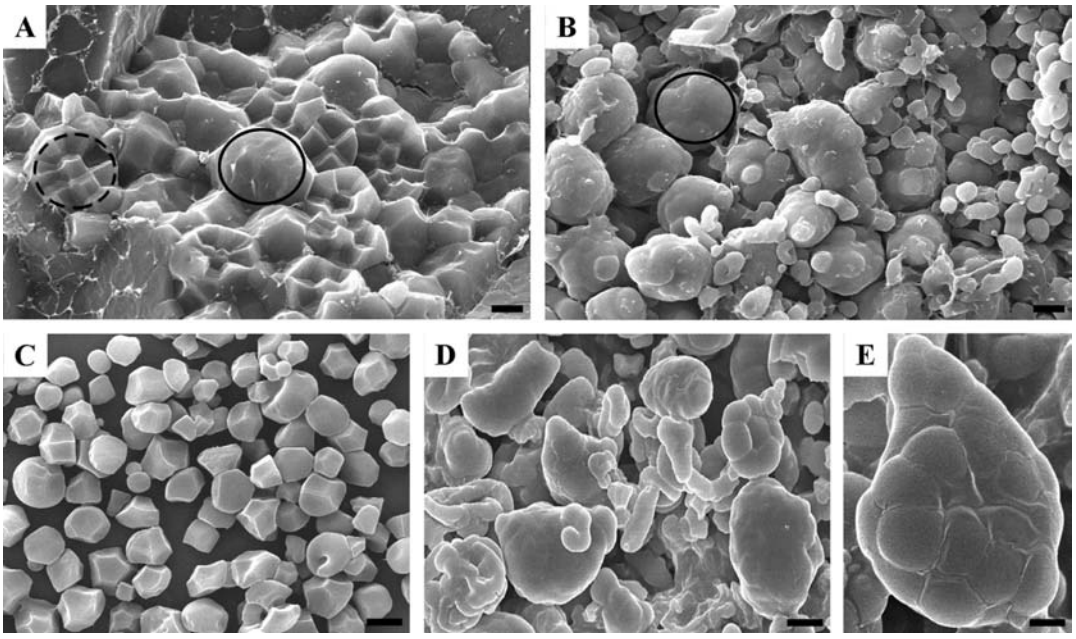

Figure 4. SEM micrographs of starch granules from TQ (**A** and **C**) and TRS (**B**, **D**, and **E**). (**A**, **B**) View of intracellularly cleaved endosperm cells in whole mature grains: (**A**) unsplit (ring) and partially split (dot ring) compound starch granules exposing the presence of individual starch granules with sharp angles and edges; (**B**) unsplit starch granules were present. Most starch granules (rings) had no sharp angles or edges with large voluminous bodies. Some small starch granules were irregular and elongated. (**C**−**E**) Morphology of starch granules isolated from mature grains: (**C**) entire population consisted of well-separated individual starch granules of similar sizes that were polygonal in shape with sharp angles and edges; (**D**) irregularly large voluminous starch granules and sausage-like elongated small starch granules; (**E**) the surface of the large voluminous starch granule was not smooth but had irregular undulations, protrusions, and linear divisions. Scale bar = 5 μm.

interior of the starch granules and the band encircled the entire circumference of the granules (**Figure 3A2,A4,A5**). This observation was consistent with the presence of multiple tightly packed starch subgranules with a surrounding layer (**Figure 2**). The APTS staining pattern of the elongated granules revealed multiple highly fluorescent round structures, which appeared to make up the interior of these granules, with a brightly stained wall encircling the entire circumference of the granules (**Figure 3A3**). This observation was consistent with the presence of multiple hila arranged like a string of pearls inside the elongated structure (**Figure 2B-③**) and suggested that aberrant initiation of new granules could be the cause of this phenomenon. CLSM optical sections of an irregularly shaped starch granule with hollow interior showed an intensely stained interior and brightly stained band encircling the entire circumference of the granules (**Figure 3A6**). This observation was consistent with the results of FM (**Figure 2B-②**) and suggested that irregularly shaped starch granules with hollow interior had higher AC. **Figure 3B**−**D** shows the CLSM serial optical sections of different shapes of TRS starch granules, which indicates the structure of starch granules and the distribution of amylose.

SEM Study of Starch Granules. The transversely fractured surface of the midregion in whole raw grains of both TQ and TRS displayed two types of endosperm cell morphology depending upon the cleavage planes, intercellular cleavage and intracellular cleavage. Intracellular cleavage of TQ endosperm produced an uneven and rough surface morphology due to the exposure of unevenly cleaved starch granules of various sizes and shapes (**Figure 4A**). Individual starch granules (ISGs) were polygonal and clustered into compound starch granules (CSGs). CSGs were either unsplit or partially split (**Figure 4A**). No partially split CSGs were detected in intracellular cleavage planes of TRS grains. Most of them were large voluminous starch granules and had no sharp angles and edges, while some of them were smaller irregular or elongated granules (**Figure 4B**). This suggested that most TRS starch granules were physically tolerant of the mechanical impact of fracturing, and thus their initial sizes and shapes remained unchanged when endosperm cells were intracellularly cleaved.

Isolated starch granules from TQ were polygonal with sharp angles and edges. The surfaces of the granules were smooth and flat or slightly concave with no structural debris (**Figure 4C**), indicating that the isolation preparation consisted primarily of pure starch subgranules. The whole or partially split CSGs presented in fractured whole grains (**Figure 4A**) were not present, indicating that the entire populations of the CSGs were totally dissociated during the isolation processes and ISGs tightly packed within them were all released freely. In contrast with those in TQ, the isolated TRS starch granules were heterogeneous in size and shape and could be grouped into two populations: one with those having smaller sizes and irregular shapes, like filamentous structures, and the other, the major population of the two, those with large voluminous bodies having roughly spherical or ovoid profiles (**Figure 4D**). These starch granules were morphologically similar to those shown in fractured whole grains (**Figure 4B**). This suggested that the starch granules of TRS endosperm cells had survived the severe treatments received during the isolation process, thereby retaining their structural integrity. In addition, the surfaces of these large voluminous starch granules were, unlike the smaller granules, not smooth but had irregular undulations and/or protrusions of various shapes and sizes (**Figure 4E**), suggesting that these were caused by the presence of solid structures of some sort in the interior of the voluminous bodies. Although these interior structures were believed to be the subgranules of TRS starch granules, it was still uncertain ultrastructurally, because the voluminous bodies were the images of

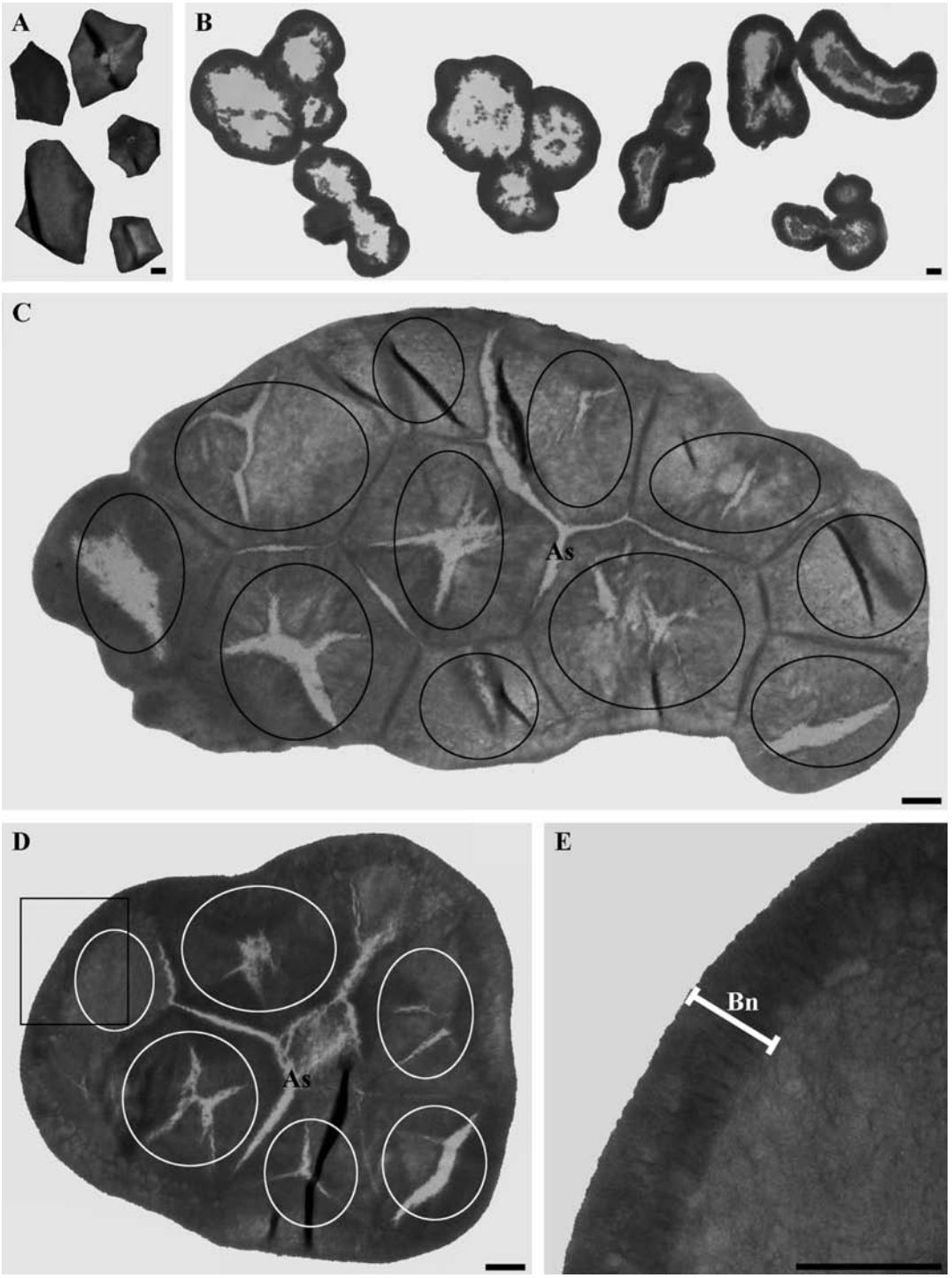

Figure 5. TEM micrographs of isolated starch granules from TQ (**A**) and TRS (**B**−**E**). (**A**) View of starch granules with polygonal shape having sharp angles and edges. (**B**) View of starch granules with irregular shape having no sharp angles and edges. The peripheral region of the granules was densely stained, but the interior was lightly stained or hollow. (**C** and **D**) View of the large voluminous starch granules with roughly spherical or ovoid shape having no sharp angles and edges. The band (Bn) encircling the entire circumference of starch granule was densely stained, and the interior consisted of tightly packed individual starch granules (ISG), demonstrating that they were indeed semicompound starch granules (SCSG). ISGs within each SCSG were separated from the adjacent ones by an electron-lucent, linear air space (As). The spaces separating ISGs were not continuous all the way through the outer surface of the granules but stopped at a short distance underneath the surface, creating a dense, continuous band (Bn) or wall encircling the entire circumference of the granule. (**E**) Higher magnification view of the squared area shown in **Figure 5D**, showing the ultrastructure of the band (Bn) encircling the entire starch granule. Scale bar = 1 μm.

their surface examined by SEM, which showed no details of internal organization of the bodies.

TEM Study of Starch Granules. Figure 5A shows several well-isolated TQ starch granules. The granules had sharp angles and edges with linear boundaries (**Figure 5A**), similar to those shown in isolated starch granules examined with LM, FM, CLSM, and SEM. The matrix of the granules was homogeneously smooth and flat with no noticeable structural

modifications or signs of the presence of non-starch material (**Figure 5A**). **Figure 5B−D** shows a low magnification view of an area where several starch granules in an isolation preparation of TRS starch were grouped. Sections of smaller irregular starch granules showed that the interiors were hollow or lightly stained, while the circumferences were heavy stained (**Figure 5B**). Sections of large voluminous starch granules showed that starch granules contained many subgranules. These subgranules packed within starch granules were separated from the adjacent ones by a thin electron-lucent linear space, apparently an air space. The spaces separating subgranules that were located at the periphery of starch granule were always oriented radially extending from the central area to the granule surface (**Figure 5C,D**). However, these radially oriented spaces did not reach through to the external surface of starch granules but stopped a short distance underneath the surface, creating externally a thick, dense, and continuous band surrounding the entire circumference of starch granule (**Figure 5C,D**). It was suggested that the starch granules, tightly appressed by the adjacent ones located internally below the circumference, participated in the formation of the band of starch granule. In a higher magnification view, the peripheral region exhibited the structural details of the band that surrounded the entire circumference of each granule (**Figure 5E**). The band consisted of radially oriented filaments aligned side by side appearing like "skeletal" elements of a starch granule, which may responsible for determining its shape, which was roughly spherical. Some interior subgranules of TRS starch granule had fissures or cracks (**Figure 5C,D**), but the TQ starch granules showed no fissures or cracks.

DISCUSSION

Starch granules are synthesized in amyloplasts and can be classified as simple, compound, and semicompound granules, depending on the number of starch granules initiated in each amyloplast (*23*). A simple granule is formed when only one granule is initiated in an amyloplast. In contrast, CSGs are composed of several separate parts, known as subgranules or granules, which come simultaneously within a single amyloplast, but each separate granule still exhibits a polarizing cross. During grain milling, the CSGs can be broken up into separate subgranules. Semicompound granules also begin as CSGs, but several separate subgranules are fused together by a surrounding layer of amorphous starch. Thus one semicompound granule always contains one exterior surface but two or more hila (*23*). In rice grains, starch granules develop in the amyloplasts of endosperm cells and form as CSGs at maturity. In each CSG, 20−60 ISGs are tightly packed (*24*). In the present study, when starches from grains were subjected to the isolation and purification processes, the products of TQ and TRS showed striking differences. The starch granules in TQ grains were completely dissociated (broken) and the ISGs were freely released. These released ISGs exhibited the typical polarizing cross under polarized light (**Figures 1** and **2**), so the starch granules in TQ grains are organized as typical CSGs. However, in TRS grains, the isolated starch granules were structurally intact, similar to that of fractured endosperm cells in the whole grains. The TRS starch granules consist of many small subgranules, some of which are located at the periphery of starch granules, fuse to each other, and form a thick band or wall encircling the entire circumference of the granules. These bands may prevent the release of subgranules during physical fracturing and/or chemical treatments. Therefore, these starch granules should be regarded as semicompound starch granules.

The hilum, which is the core of the granule and the starting point from which the granule grows, is commonly situated near the middle of the granule, but it can be eccentric, i.e., toward one end of the granule (*25*). The shape of hilum may be in the form of a point, stellate and radiating from the center, or elongated and branched. Central vacuoles (also known as open hila) are also found in some species (*25*). Normal rice starch granules show a concentric point hilum (*26*). In high-amylose TRS, most hila are clear in the middle of subgranules. Some elongated starch granules showed multiple hila arranged like a string of pearls inside granules. Some large voluminous starch granules appeared to contain multiple hila. These phenomena were also reported in high-amylose starch granules from maize (*26*). Light microscopic observation showed that, in the SGP-1 null wheat with apparent high amylose, large starch granules were mostly deformed, and their hila appeared to be cracked. SEM showed that the hila of the deformed granules were hollow (*27*). The starch in high-amylose potato lines had a shape resembling that of normal starch granules; however, the surface was irregular, and many of the granules possessed asymmetrical fissures and were generally not birefringent as viewed under polarized light (*21*, *26*). Starch granules with suppressed SBE had severe internal cracks and rough surfaces (*21*). A study of high-amylose maize by Atkin et al. (*28*) showed that the round maize granules were normally birefringent, whereas the elongated structures were only weakly birefringent at the surface, indicating a lack of internal crystalline order. Blennow et al. (*21*) reported that fissures and cracks were detected in the antisense SBE potato starch granules, but birefringence (maltese cross) effects were clearly visualized. The cracks did not result in a dramatic change in form of the birefringence pattern. Hence, growth of these granules most likely continued at the surface of the granule after cracking (*21*). In this study, we could not observe the fissure or cracks in the high-amylose TRS starch granules under light microscopy but did inside the starch subgranules under TEM. This might be that the starch granules were too small to observe the fissure cracks under light microscopy. The birefringence of TRS granules, especially of the elongated and filamentous starch granules, was considerably weaker and resulted in a lower contrast between birefringence and background when compared to that of TQ granules. This effect would likely be a result of the high amylose (low amylopectin) concentrations in these starch granules since amylose molecules are not expected to be specifically uniformly oriented in the granule (*21*).

It has been demonstrated that the synthesis of amylose occurs inside the granule (*29*). In native starch granules, amylose appears to be interspersed among the amylopectin molecules (*30*). Previous reports have suggested that amylose is quite concentrated near the granule surface (*31*). Data from enzyme-gold labeling experiments and iodine staining of hydrated maize and potato granules indicate that amylose is localized in distinct amorphous regions around the hilum (*28*). Under CLSM coupled with the unequal APTS fluorescence distribution between amylose and amylopectin, the internal structures could be visualized, and thus we could understand the relation between the internal structures and shape and surface of the granule. Analysis of APTS-labeled potato granules demonstrated the preferential labeling of amylose and showed that the fluorescence intensity as imaged by CLSM was positively correlated to amylose content (*21*). Normal potato amylose granules showed an intense approximately 1 μm large fluorescence dot in the hilum, indicating a high concentration of amylose in the center of the granule (*21*). In high-amylose maize and potato, the irregular granule shapes could be observed, and there presented multiple round fluorescent structures. In maize, these granules were often elongated, and the filamentous

structures with the fluorescent bodies are arranged like a string of pearls inside the elongated structures (*26*). The high-amylose phenotype of Amo1 gave rise to obvious, large glowing cores (*32*). The results of this study showed that the regular TQ starch granules have an intense fluorescence in the concentric hilum, indicating a high concentration of amylose in the center of the granules. In the case of TRS starch granules, there was a relatively even distribution of high fluorescence but intense fluorescence in the hilum and wall encircling the entire circumference of the granules.

In conclusion, with a result of high amylose by simultaneous inhibition of expression of two SBEs in transgenic rice endosperm, there are great effects on either the microstructure or ultrastructure of the starch granules, when comparing with those of regular rice. In the grains of the high-amylose rice TRS, the starch granules tend to form large voluminous and non-angular rounded or elongated and filamentous structures and are structurally intact and very tolerant to fracturing. However, the granules from the regular rice TQ are organized as CSGs and are easily dissociated to separate ISGs during fracturing. The semicompound starch granules from TRS grains consist of packed small subgranules, some of which fuse to each other and form a thick wall encircling the entire circumference of the granules. Moreover, under the CLSM coupled with APTS fluorescence staining, inside the TRS granules there was intense amylose not only in the hilum but also the wall of the semi-CSGs. It is different from that in TQ granules, in which the intense amylose is only present in the granule hilum. These data are helpful to understand the formation of high amylose in TRS endosperm as well as for further application of high-amylose RS rice in food and nonfood industry.

ABBREVIATIONS USED

AAC, apparent amylose content; AC, amylose content; BFM, bright field microscopy; CLSM, confocal laser scanning microscopy; CSG, compound starch granule; FM, fluorescent microscopy; ISG, individual starch granule; LM, light microscopy; PLM, polarized light microscopy; RS, resistant starch; SBE, starch branching enzyme; SCFA, short chain fatty acid; SEM, scanning electron microscopy; TEM, transmission electron microscopy.

LITERATURE CITED

(1) Englyst, H.; Kingman, S.; Cummings, J. Classification and measurement of nutritionally important starch fractions. *Eur. J. Clin. Nutr.* **1992**, *46*, S33–S50.

(2) Topping, D. L.; Clifton, P. M. Short-chain fatty acids and human colonic function: roles of resistant starch and nonstarch polysaccharides. *Physiol. Rev.* **2001**, *81*, 1031–1064.

(3) Jacobasch, G.; Schmiedl, D.; Kruschewski, M.; Schmehl, K. Dietary resistant starch and chronic inflammatory bowel diseases. *Int. J. Colorectal Dis.* **1999**, *14*, 201–211.

(4) Govers, M. J.; Gannon, N. J.; Dunshea, F. R.; Gibson, P. R.; Muir, J. G. Wheat bran affects the site of fermentation of resistant starch and luminal indexes related to colon cancer risk: a study in pigs. *Gut* **1999**, *45*, 840–847.

(5) Higgins, J. A.; Brand Miller, J. C.; Denyer, G. S. Development of insulin resistance in the rat is dependent on the rate of glucose absorption from the diet. *J. Nutr.* **1996**, *126*, 596–602.

(6) Younes, H.; Remesy, C.; Behr, S.; Demigne, C. Fermentable carbohydrate exerts a urea-lowering effect in normal and nephrectomized rats. *Am. J. Physiol.* **1997**, *272*, 515–521.

(7) Murphy, M. M.; Douglass, J. S.; Birkett, A. Resistant starch intakes in the United States. *J. Am. Diet. Assoc.* **2008**, *108*, 67–78.

(8) Ito, T.; Saito, K.; Sugawara, M.; Mochida, K.; Nakakuki, T. Effect of raw and heat-moisture-treated high-amylose corn starches on the process of digestion in the rat digestive tract. *J. Sci. Food Agric.* **1999**, *79*, 1203–1207.

(9) Schwall, G. P.; Safford, R.; Westcott, R. J.; Jeffcoat, R.; Tayal, A.; Shi, Y. C.; Gidley, M. J.; Jobling, S. A. Production of very-high-amylose potato starch by inhibition of SBE A and B. *Nat. Biotechnol.* **2000**, *18*, 551–554.

(10) Bird, A. R.; Jackson, M.; King, R. A.; Davies, D. A.; Usher, S.; Topping, D. L. A novel high-amylose barley cultivar (*Hordeum vulgare* var. Himalaya 292) lowers plasma cholesterol and alters indices of large-bowel fermentation in pigs. *Br. J. Nutr.* **2004**, *92*, 607–615.

(11) Regina, A.; Bird, A.; Topping, D.; Bowden, S.; Freeman, J.; Barsby, T.; Kosar-Hashemi, B.; Li, Z.; Rahman, S.; Morell, M. High-amylose wheat generated by RNA interference improves indices of large-bowel health in rats. *Proc. Natl. Acad. Sci. U.S.A.* **2006**, *103*, 3546–3551.

(12) Frei, M.; Siddhuraju, P.; Becker, K. Studies on the in vitro starch digestibility and the glycemic index of six different indigenous rice cultivars from the Philippines. *Food Chem.* **2003**, *83*, 395–402.

(13) Yano, M.; Okuno, K.; Kawakami, J.; Satoh, H.; Omura, T. High amylose mutants of rice, *Oryza sativa* L. *Theor. Appl. Genet.* **1985**, *69*, 253–257.

(14) Kang, H. J.; Hwang, I. K.; Kim, K. S.; Choi, H. C. Comparative structure and physicochemical properties of IIpumbyeo, a high-quality *japonica* rice, and its mutant, Suweon 464. *J. Agric. Food Chem.* **2003**, *51*, 6598–6603.

(15) Yang, C. Z.; Shu, X. L.; Zhang, L. L.; Wang, X. Y.; Zhao, H. J.; Ma, C. X.; Wu, D. X. Starch properties of mutant rice high in resistant starch. *J. Agric. Food Chem.* **2006**, *54*, 523–528.

(16) Li, M.; Piao, J. H.; Liu, Q. Q.; Yang, X. G. Effects of the genetically modified rice enriched with resistant starch on large bowel health in rats. *Acta Nutr. Sin.* **2008**, *30*, 588–591.

(17) Juliano, B. O. A simplified assay for milled rice amylose. *Cereal Sci. Today* **1971**, *16*, 334–360.

(18) McCleary, B. V.; McNally, M.; Rossiter, P. Measurement of resistant starch by enzymatic digestion in starch and selected plant materials: collaborative study. *J. AOAC Int.* **2002**, *85*, 1003–1111.

(19) Takeda, Y.; Takeda, C.; Mizukami, H.; Hanashiro, I. Structures of large, medium and small starch granules of barley grain. *Carbohydr. Polym.* **1999**, *38*, 109–114.

(20) Evans, A.; McNish, N.; Thompson, D. B. Polarization colors of lightly iodine-stained maize starches for amylose-extender and related genotypes in the W64A inbred line. *Starch/Stärke* **2003**, *55*, 250–257.

(21) Blennow, A.; Hansen, M.; Schulz, A.; Jørgensen, K.; Donald, A. M.; Sanderson, J. The molecular deposition of transgenically modified starch in the starch granule as imaged by functional microscopy. *J. Struct. Biol.* **2003**, *143*, 229–241.

(22) Juliano, B. O. An international survey of methods used for the cooking and eating qualities of milled rice. *IRRI Res. Pap. Ser.* **1982**, *77*, 1–28.

(23) Shannon, J. C.; Garwood, D. L. Genetics and physiology of starch development. In *Starch: Chemistry and Technology*; Whistler, R. L., Bemiller, J. N., Paschall, E. F., Eds.; Academic Press: New York, 1984; pp 25−86.

(24) Juliano, B. O. Polysaccharides, proteins and lipids of rice. In *Rice: Chemistry and Technology*; Juliano, B. O., Ed.; American Association of Cereal Chemists: St. Paul, MN, 1985; pp 59−174.

(25) Gott, B.; Barton, H.; Samuel, D.; Torrence, R. Biology of starch. In *Ancient Starch Research*; Torrence, R., Barton, H., Eds.; Left Coast Press: Walnut Creek, CA, 2006; pp 35−45.

(26) Glaring, M. A.; Koch, C. B.; Blennow, A. Genotype-specific spatial distribution of starch molecules in the starch granule: a combined CLSM and SEM approach. *Biomacromolecules* **2006**, *7*, 2310–2320.

(27) Yamamori, M.; Fujita, S.; Hayakawa, K.; Matsuki, J.; Yasui, T. Genetic elimination of a starch granule protein, SGP-1, of wheat generates an altered starch with apparent high amylose. *Theor. Appl. Genet.* **2000**, *101*, 21–29.

(28) Atkin, N. J.; Cheng, S. L.; Abeysekera, R. M.; Robards, A. W. Localization of amylose and amylopectin in starch granules using enzyme-gold labeling. *Starch/Stärke* **1999**, *51*, 163–172.

(29) Tatge, H.; Marchall, J.; Martin, C.; Edwards, A.; Smith, A. M. Evidence that amylose synthesis occurs within the matrix of the starch granule in potato tubers. *Plant Cell Environ*. **1999**, *22*, 543–550.
(30) Jane, J.; Xu, A.; Radosavljevic, M.; Seib, P. A. Location of amylose in normal starch granules. I: susceptibility of amylose and amylopectin to cross-linking reagents. *Cereal Chem*. **1992**, 405–409.
(31) Jane, J. L.; Shen, J. J. Internal structure of the potato starch granule revealed by chemical gelatinization. *Carbohydr. Res*. **1993**, *47*, 279–290.
(32) Borén, M.; Glaring, M. A.; Ghebremedhin, H.; Olsson, H.; Blennow, A.; Jansson, C. Molecular and physicochemical characterization of the high-amylose barley mutant Amo1. *J. Cereal Sci*. **2008**, *47*, 79–89.

Received for review September 6, 2009. Revised manuscript received October 26, 2009. Accepted November 6, 2009. This study was financially supported by grants from the National Natural Science Foundation of China (30530470, 30300215, 30828021), the National Major Special Project for the Development of Transgenic Organisms (2008ZX08009−003, 2009ZX08011−003B), the Natural Science Foundation of Jiangsu (BK2009186, BK2007510), and the China Postdoctoral Science Foundation (20090451252).